IASMiRT

SMiRT 26
50 Anniversary Berlin/Potsdam

Transactions, SMiRT-26
Berlin/Potsdam, Germany, July 10-15, 2022
Division I

MODELING CONCRETE EXPANSION DUE TO ALKALI-SILICA REACTION

Gunay Gina Aliyeva[1], Yann Le Pape[2], Abhinav Gupta[3], Sujit Samaddar[4]

[1]PhD Student, Center for Nuclear Energy Facilities and Structures, NCSU, USA (ggaliyev@ncsu.edu)
[2]Oak Ridge National Laboratory, Oak Ridge, TN, USA
[3]Director, Center for Nuclear Energy Facilities and Structures, NCSU, USA
[4]US Nuclear Regulatory Commission, USA

ABSTRACT

Alkali-silica reaction (ASR) in concrete is a chemical reaction that leads to a reduction in the structural performance of nuclear power plant concrete structures and causes millions of dollars worth of damage. The process can cause serious cracks over multiple decades, and hence, it is important to understand and investigate the mechanism of the ASR-affected concrete. This study follows the assumption of a volumetric expansion due to ASR and the redistribution of the volumetric expansion depending on the state of stress in the concrete. In this paper, ASR-affected concrete expansion is investigated using a new approach by coupling the chemical and physical mechanisms to calculate the total strains of an ASR-affected structure considering the anisotropy of the expansion and the creep effect. The main contribution of this approach is that it updates the mechanical and creep strains of a structure depending on the damage due to ASR. Experimental data from ASR-affected concrete cylinder specimens with different states of stress are used to verify the approach. Through this approach, it is possible to determine the progression of strains in the ASR-affected concrete structures and determine their loss of strength over multiple decades.

INTRODUCTION

Alkali-silica reaction (ASR) in concrete is a slow-evolving chemical reaction between the reactive silica in the aggregate and the alkali in concrete that produces a gel inside the concrete. The gel expands and increases in volume in the presence of sufficient moisture. Expansion of the gel causes cracking and loss of strength in the concrete. The damage in nuclear structures is highly undesirable as it can require shutting down of power plants for maintenance which leads to significant economic loss. Expansion of the gel can lead to significant cracking that can cause degredation in mechanical properties of the concrete (Commission, 2011). Thus, it is important to investigate the mechanism of ASR-affected concrete. This study proposes a new approach to simulate the ASR-induced expansion in concrete by using a chemo-damage constitutive model.

Past research explores the ASR-induced expansion mechanism with the assumption of a volumetric expansion of the gel and shows that the total volumetric ASR-induced strain is almost constant, irrespective of the confinement. Larive (1998) tested more than 600 specimens with uniaxial confinement to show that the volumetric ASR-induced strains are almost constant. Multon and Toutlemonde (2006) illustrated the existence of constant volumetric strain further by testing concrete specimens under the triaxial state of stress. Saouma and Perotti (2006) developed a constitutive model to define ASR-induced expansion. Their model considers the chemistry, physics, and mechanics of the concrete by including retardation, the kinetics of ASR, and the humidity effect in the volumetric strain calculation. Moreover, there is strong evidence of a volumetric expansion transfer and that the expansion is largest in the direction of least resistance whereas

it is reduced in the loading direction. Saouma and Perotti (2006)'s model introduced the expansion transfer in terms of weights and included the expansion redistribution for the first time.

In this study, a new approach is used to investigate the ASR-affected concrete expansion by including the ASR-induced damage and coupling the chemical and physical mechanisms. The proposed approach updates the mechanical and creep strains of a structure depending on the damage due to ASR which is the main contribution of this approach. Total strains of ASR-affected specimens were calculated and results are compared with different models as well as the experimental study. The proposed method makes it possible to determine the progression of strains in the ASR-affected concrete structures and represent the anisotropic expansion accurately.

PROPOSED APPROACH

Volumetric ASR-induced Strain

Past research defined the general uncoupled ASR-induced equation for the incremental volumetric ASR-induced strain by Equation 1 (Saouma and Perotti, 2006). As shown in Equation 1, volumetric expansion is defined as a function of, Γ_t, the ASR−induced reduction due to tensile cracking, Γ_c, the reduction in ASR−induced volumetric expansion under compressive stresses, $f(h)$, humidity effect, $\xi(t,T)$, ASR extent which is a sigmoid curve expressing the volumetric expansion in time as a function of temperature, and $\varepsilon^{\infty}_{ASR}$, the laboratory−determined maximum free volumetric expansion at the reference temperature.

$$\varepsilon^{ASR}_{vol} = \Gamma_t \Gamma_c f(h) \xi(t,T)\, \varepsilon^{\infty}_{ASR} \tag{1}$$

There is also a simplified version of the volumetric strain calculation in literature (Pan et al., 2013) which defines the volumetric ASR−induced strain as a function of $f(h)$, $\xi(t,T)$, and $\varepsilon^{\infty}_{ASR}$ and couples it with the ASR−induced damage and mechanical damage (Equation 2). As shown in Equation 3, the ASR extent, $\xi(t,T)$, is defined as a function of T_C and T_L which are the characteristic time and the latency time of expansion, respectively. Humidity effect, $f(h)$, was taken as 1 considering that there will be enough moisture. The proposed approach in this study considers volumetric ASR−induced expansion and calculates volumetric strain and ASR kinetics , as seen in Equation 2 and Equation 3.

$$\varepsilon^{ASR}_{vol} = f(h)\xi(t,T)\varepsilon^{\infty}_{ASR} \tag{2}$$

$$\xi(t,T) = \frac{1 - e^{-\frac{t}{T_C(T)}}}{1 + e^{-\frac{t - T_L(T)}{T_C(T)}}} \tag{3}$$

Expansion Transfer

The reduced expansion in the loaded directions and increased expansion in the unconstrained ones in the previous experiments led Saouma and Perotti (2006) to introduce weights for the expansion redistribution. Expansion redistribution was accomplished by assigning weights to each of the three principal directions.

Weights were determined through a bilinear interpolation for the given state of stress and material properties of the specimen. Following this assumption, the expansion model will indeed result in an anisotropic expansion. ASR−induced strain in each principal direction is calculated using Equation 4 where W_i represents the calculated weight for the given direction. Based on Larive (1998)'s study, it was assumed that no ASR expansion occurs at pressures above 10 MPa. This study follows Saouma and Perotti (2006)'s weight definition and the assumption of expansion redistribution among principal directions depending on the state of stress.

$$\varepsilon_i^{ASR} = W_i \varepsilon_{vol}^{ASR} \tag{4}$$

ASR-induced Damage: d_{ASR}

The ASR−induced expansion causes a change in the mechanical characteristics of the concrete. It can be assumed that the expansion creates damage and changes the stiffness of the structure. The relationship between ASR−induced expansion and tension damage was investigated by Capra and Sellier (2003) and the damage factor in tension, d_{ASR}, was calculated by determining the probabilities of cracking. According to this study, ASR plastic strains can be defined as a function of the damage factor (refer to Equation 5). As shown in Equation 6, the change in Young's modulus can be defined in terms of d_{ASR} where E_o and E represent the initial and current Young's moduli, respectively.

$$\varepsilon_i^{ASR} = 0.003 \frac{d_{ASR}}{1 - d_{ASR}} \tag{5}$$

$$\frac{E}{E_o} = 1 - d_{ASR} \tag{6}$$

Strains due to External Loads

As shown in Equation 6, damage due to ASR changes the elastic stiffness, and hence, mechanical strains due to external loads should be updated accordingly for each time step. Updated mechanical strain ($\varepsilon_{mech}^{updated}$) can be calculated for each principal direction using Equation 7 for cases where external loads are less than the strength of the concrete. ε_{mech} is the constant mechanical strain due to external loading, ignoring the creep effect.

$$\varepsilon_{mech}^{updated} = \frac{\varepsilon_{mech}}{1 - d_{ASR}} \tag{7}$$

Creep Strains

The creep strains (ε_{ve}) are part of the total strain calculation and coupled with the damage effect. The mechanical strains including the creep effect ($\varepsilon_{ve} + \varepsilon_{mech}$) can be modeled for any structure using different methods without considering the ASR effect. But it is possible to update the creep model depending on the ASR−induced damage. In this study, it's assumed that the damage due to ASR affects the creep strains so Equation 8 is presented to consider this coupled mechanism and calculate the updated creep strains.

$$\varepsilon_{ve}^{updated} = \frac{\varepsilon_{ve} + \varepsilon_{mech} - \varepsilon_{mech}^{updated}}{1 - d_{ASR}} \tag{8}$$

Shrinkage Strains

The shrinkage strains (ε_{sh}) are also part of the total strain calculation and are not coupled with the damage effect in the proposed approach. These strains can be obtained from measurements of not loaded "creep and shrinkage only" (non-reactive) specimens which don't experience ASR and ASR−induced expansion.

Total Strain

The total strain in each principal direction will be the combination of the mechanical strains, creep strain, shrinkage strain, and ASR−induced strain in that direction. Total strain calculation for the new approach is shown in Equation 9 for the direction i.

$$(\varepsilon_{total})_i = \varepsilon_i^{ASR} + (\varepsilon_{mech}^{updated})_i + (\varepsilon_{ve}^{updated})_i + (\varepsilon_{sh})_i \tag{9}$$

VERIFICATION

Multon and Toutlemonde's Tests

Multon and Toutlemonde (2006) studied the ASR-induced expansion with accelerated tests by investigating concrete cylindrical specimens subjected to different states of stresses among the principal directions. They measured the applied stresses and resulting strains of the specimens for over 500 days until the ASR−induced strains were almost constant for the specimens. ASR−induced axial and radial strains were plotted for 130 by 240 mm cylinder specimens subjected to all combinations of three axial compressive stresses (0, 10, 20 MPa) and three transverse confining levels (0, 3, 5 mm). The results from three cases were used to do the verification of the coupled approach in this study: Case 1, a free expansion case with no load and no confinement, Case 2, a uniaxially loaded case with 10 MPa axial load and no confinement, and Case 3, a uniaxially loaded case with 20 MPa axial load and no confinement. These cases are presented in Figure 1. Young's modulus of concrete (E_o) was taken as 37300 MPa and Poisson's ratio (ν) was measured as 0.22 for the specimens.

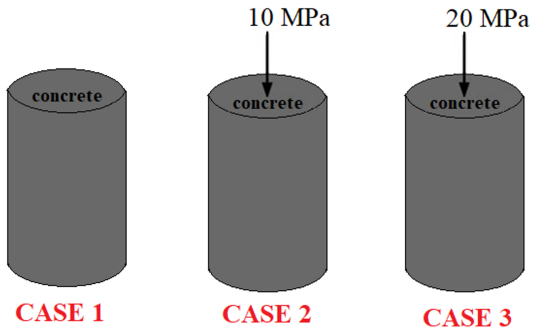

Figure 1. Three cases used for the verification

Comparison

Pan et al. (2013) proposed a coupled chemo−damage model by including the damage due to ASR as well as the mechanical damage of the concrete in their constitutive model. They used Multon and Toutlemonde (2006)'s experimental results to verify their model and presented the ASR−induced strains for the same cases (Cases 1, 2 and 3). Morenon et al. (2017) also studied the same cases and described the impact of applied stresses on ASR expansion and ASR−induced anisotropic cracking. They obtained the cracks using the principles of poromechanics, and induced the anisotropy in their model by the equilibrium between stress and the gel pressure. They presented total strains and compared their results with the experimental results. The models in these studies are based on different techniques but tries to achieve the same goal which is to represent the experimental behavior accurately. The results from Pan et al. (2013), Morenon et al. (2017) and, experimental study (Multon and Toutlemonde, 2006) will be compared with the proposed approach's results for the three cases given in Figure 1.

APPLICATION

Case 1: Free Expansion

One of the tested cylinders which is used for the verification and also for the initial calibration is the free expansion case. This specimen doesn't have any constraints or load on it and was observed for over 500 days to capture the free expansion due to ASR. Axial and radial strains were measured throughout the experiment and are shown in Figure 2a and Figure 2b, respectively. Experimental radial strains of free expansion in Figure 2b were used to find the parameters of ASR kinetics by inverse analysis. Latency and characteristic times were obtained as 120 days and 60 days, respectively. Maximum free volumetric expansion, $\varepsilon^{\infty}_{ASR}$, was taken as 0.0026.

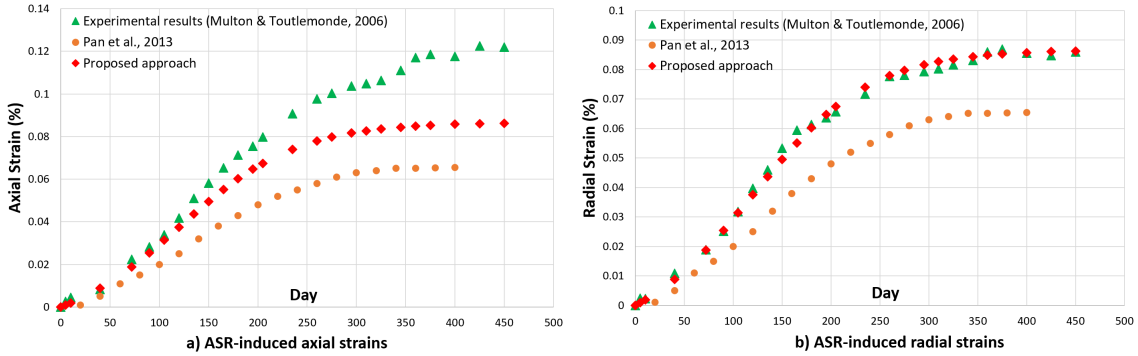

Figure 2. ASR-induced strains for Case 1 (free expansion)

Using Equation 2 and Equation 3, volumetric ASR−induced strains were calculated for every time step where we have the experimental measurement. Since it is a free expansion case, it can be assumed that all the principal directions will equally share the volumetric ASR−induced strain (isotropic expansion), and hence, weights will be equal for the axial and radial directions. Volumetric ASR−induced strains were distributed among the principal directions using Equation 4 and assuming that the weight for the axial direction, W_{axial} is 1/3, and the weight for the radial direction, W_{radial} is 1/3. Axial and radial strains (only caused by ASR) were shown in Figure 2a and Figure 2b to compare them with the experimental results as well as Pan et al. (2013)'s model. Higher axial strains were observed in the experiments because of the casting direction (Multon and Toutlemonde, 2006). And hence, this difference is not considered in the proposed approach due to the isotropic free expansion assumption. This is a fair assumption to make and was followed by many studies in the literature.

Pan et al. (2013) also used the same isotropic expansion assumption but calculated lower radial and axial strains, because their calibration wasn't based on "only ASR−induced" strains but also includes the shrinkage effect. However, the calibration of ASR parameters should be done after fitting creep and shrinkage on no ASR (non−reactive) material. And later on, Pan et al. (2013)'s model didn't include the shrinkage effect. However, shrinkage is an important effect on both axial and radial directions as observed in the experiments of non−reactive models.

This case is an appropriate example to calibrate a model and also observe the "only ASR−induced strains" in a specimen. Since there is no load or constraint on the specimen, the strains calculated for this case were the ASR−induced axial and radial strains only. Thus, the effect of ASR−induced damage can't be seen in this case.

Creep & Shrinkage

An important effect to consider in this approach is the creep effect. ASR effect occurs for a long time and hence, the effect of creep should be taken into account. The experimental study presents results for the same cases with creep and shrinkage only specimens (non−reactive) which helps us to obtain the pure shrinkage and creep effect for the same cases where no ASR−induced expansion was expected. Experimental measurements for the creep and shrinkage only specimens for these 3 cases are given in Figure 3 for both axial and radial directions.

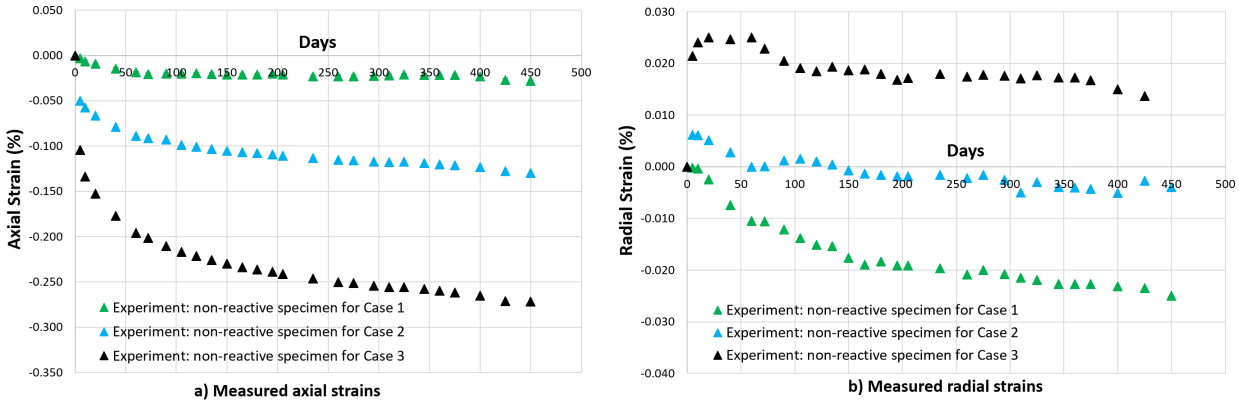

Figure 3. Experimental strain measurements for creep and shrinkage only specimens

The strains in Figure 3 show the combination of mechanical strain, creep strain, and shrinkage strain. Since these specimens can only have creep and shrinkage, Case 1 with zero loads has no creep or mechanical strain. Thus, axial and radial strains for Case 1 are only caused by shrinkage and these strains were used as shrinkage strain (ε_{sh}) in this study. It was shown that shrinkage strain was almost constant (-0.02%) after some time. In Figure 3, Cases 2 and 3 consider axial load and creep effect. So the measured strains are given for the combination of the mechanical strains including the creep effect ($\varepsilon_{ve} + \varepsilon_{mech}$) as well as the shrinkage strain (ε_{sh}). We should note that these measurements don't include the ASR effect and ASR−caused damage. In the presented approach, the shrinkage behavior given here will be used as the constant shrinkage strain, and the creep model will be used by combining it with the ASR−induced damage.

Case 3 - No creep / No shrinkage

Before investigating Case 2, we will compare Case 3 with a model from past research by ignoring the creep and shrinkage effect. Case 3 doesn't have a radial constraint to prevent the expansion in the radial direction. However, the axial direction has a 20 MPa load which creates a more complex behavior compared to Case 1. It's possible to observe the assumption of expansion transfer for this case.

In the proposed approach, the volumetric ASR−induced strains were calculated for every time step, the same way as in Case 1. 20 MPa load on the specimen will restrict the ASR−induced expansion in the axial direction. According to the expansion transfer assumption, the volumetric strain will be distributed among the other 2 directions. Thus, the volumetric ASR−induced strains were distributed using Equation 4 and assuming that the weight for the axial direction, W_{axial} is 0, and the weight for the radial direction, W_{radial} is 1/2. This calculation helps us to find ASR−induced strain, ε_i^{ASR} in both axial and radial directions. However, this strain won't be the only ASR−induced strain. The specimen has a 20 MPa axial load and when ignoring creep, the axial load can be taken as a constant load for each time step. As shown in Equation 6, damage due to ASR changes the elastic stiffness. Thus, the updated strains ($\varepsilon_{mech}^{updated}$)

due to 20 MPa for each t day was calculated using Equation 7 which includes the effect of ASR−induced damage. The total updated strain, $(\varepsilon_{total})_i$ for this case is calculated using Equation 10 which combines the mechanical strain due to 20 MPa (coupled with ASR−induced damage) with the ASR−induced strain from the expansion transfer of the volumetric strain. Purely ASR−induced strain then was calculated by subtracting the constant strain due to mechanical load from the total strain as given in Equation 11 and plotted in Figure 4.

The only coupled mechanism introduced here is between the mechanical strains and the damage due to ASR. The strains for the presented approach in this study, the strains from Pan et al. (2013)'s model, the strains from Morenon et al. (2017)'s model, and the experimental results are compared in Figure 4 for the axial and radial directions. Pan et al. (2013) obtained the ASR−induced strains for Case 3 without adding the creep effect. Morenon et al. (2017) showed the total strains as well as creep shrinkage strains for the same case. We calculated "only ASR−induced strains" for Morenon et al. (2017)'s model by subtracting the strains of their creep and shrinkage model from the total strains of their model. Results from Morenon et al. (2017)'s model were approximately taken from their study.

$$(\varepsilon_{total})_i = \varepsilon_i^{ASR} + (\varepsilon_{mech}^{updated})_i \tag{10}$$

$$(\varepsilon_{ASR}^{updated})_i = (\varepsilon_{total})_i - (\varepsilon_{mech})_i \tag{11}$$

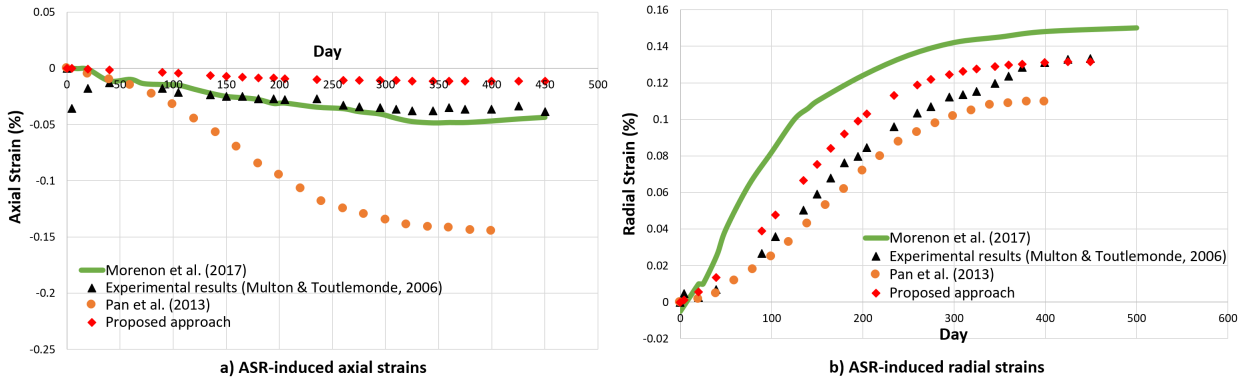

Figure 4. Only ASR-induced strains for Case 3 (no creep / no shrinkage)

The experimental study (Multon and Toutlemonde, 2006) presents measurements for "only creep and shrinkage" (non−reactive) specimens (where there is no ASR expansion) as well as for the ASR included (reactive) specimens. The experimental "only ASR−induced strains" for Case 3 were obtained by subtracting the measured strains of the only creep and shrinkage (non-reactive) specimen from the strains of the ASR included (reactive) specimen.

Axial and radial strains of the proposed approach show good agreement with the experimental results. Morenon et al. (2017) obtained the cracks using the principles of poromechanics and induced the anisotropy in their model by the equilibrium between stress and ASR−gel pressure. Although their model is based on different technique, it shows good agreement for the axial direction as seen in Figure 4. However, radial strains were higher for Morenon et al. (2017)'s model compared to the proposed approach. As seen in Figure 4, the proposed approach's radial strains fit better with the experimental data. Pan et al. (2013) included the mechanical damage in their model and the strains from their model overestimates the ASR−induced strains in the axial direction. Pan et al. (2013)'s model match better in the radial direction. However, this is not important as the axial strains are very unrealistic.

The proposed approach that includes the coupled effect between ASR−induced damage and mechanical strains gives more realistic axial and radial strains. This also proves that the volumetric ASR−induced strains are not transferred in the axial direction as the weight is zero for the axial direction according to Saouma and Perotti (2006)'s expansion transfer study. Even with no expansion transfer in the axial direction, there is still ASR−induced strain observed in the axial direction which can be explained by the stiffness change due to ASR−induced damage.

Case 2 & Case 3 - Effect of Creep & Shrinkage

The mechanical strains including the creep effect (ε_{ve} +ε_{mech}) was calibrated without considering the ASR effect. But the creep model needs to be updated depending on the ASR−induced damage. In this study, it's assumed that the damage due to ASR affects the creep strains so the updated creep strains were measured using Equation 8 for both axial and radial directions. The shrinkage strains (ε_{sh}) are not coupled with the damage effect.

Case 2 & Case 3 - Total Strains

The total strains for each direction, $(\varepsilon_{total})_i$, were calculated using Equation 9 for both Cases 2 and 3 for the proposed approach. These results were compared with Multon and Toutlemonde (2006)'s experimental total strain measurements as well as Morenon et al. (2017)'s model. Pan et al. (2013)'s model is not included in the comparison as their no creep / no shrinkage model significantly overestimates the axial strains (refer to Figure 4) and gives highly unrealistic ASR−induced strains in the axial direction. Thus, after adding an appropriate creep&shrinkage model, Pan et al. (2013)'s results wouldn't be close to the experimental results. Morenon et al. (2017) presented the same cases, and results from their model were approximately taken from their study for Cases 2 and 3 to compare it with the proposed approach. This comparison is given in Figure 5 and Figure 6 for Cases 2 and 3, respectively. Morenon et al. (2017)'s model is based on a totally different technique and follows the principles of poromechanics and it shows good agreement in the axial direction. However, in the radial direction, Morenon et al. (2017)'s model has higher radial strains. This difference is even more significant for Case 3 where the axial load increases. As seen in Figure 5 and Figure 6, proposed approach gives better radial strain results compared to Morenon et al. (2017)'s model.

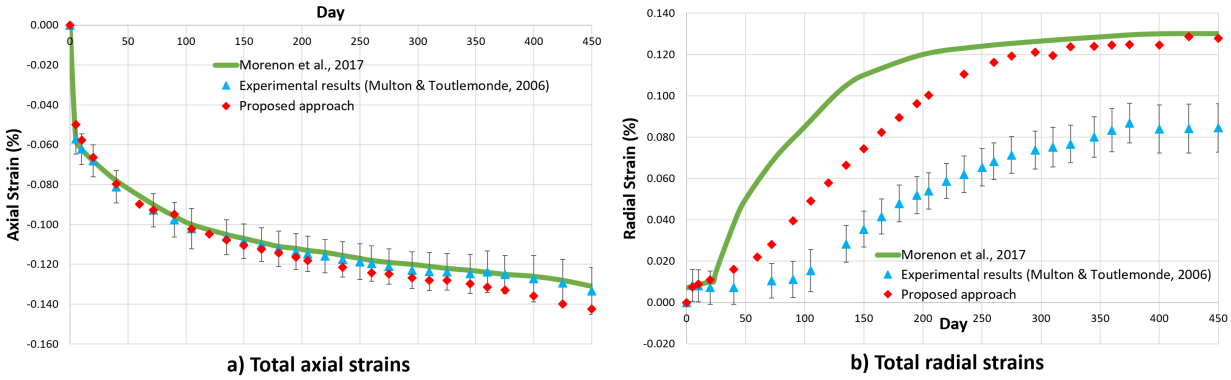

Figure 5. Total strains for Case 2

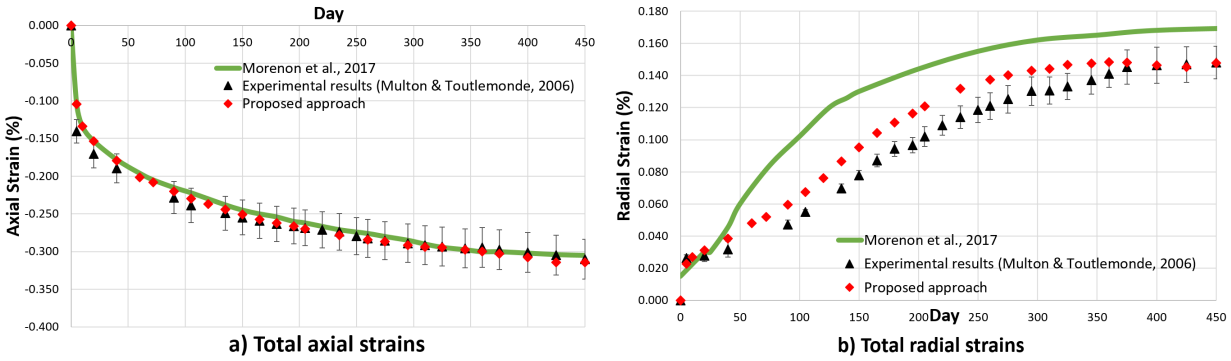

Figure 6. Total strains for Case 3

SUMMARY AND CONCLUSIONS

In this study, the effect of ASR expansion in concrete is investigated by a new approach that couples the chemical and physical mechanisms of the expansion. The main contribution of the proposed approach is that it combines the damage due to ASR with its effect on the mechanical and creep strains. The proposed approach considers the anisotropy of the expansion and the creep & shrinkage effects. Findings from the past experimental study were compared with the results of the proposed approach. The proposed approach shows good agreement with the experimental study.

It is essential to obtain the progression of strains in the ASR-affected concrete structures and determine their loss of strength over multiple decades. The proposed approach appears to be rational and accurate enough to obtain the strains due to anisotropic expansion of the ASR-affected concrete structures. Further investigation of the model parameters will help to build future numerical simulation problems.

References

Capra, B. and Sellier, A. (2003). "Orthotropic modelling of alkali-aggregate reaction in concrete structures: numerical simulations." *Mechanics of materials*, 35(8), pp. 817–830.

Commission, U. N. R. (2011). "NRC Information Notice 2011-20: Concrete degradation by alkali-silica reaction." *ML112241029*.

Larive, C. (1998). *Apports Combin'es de l Experimentation et de la Modélisation à la Comprehension del Alcali-Réaction et de ses Effets Mécaniques (in France)*. Ph.D. thesis, Dissertation of Doctoral Degree. Paris: Thése de Doctorat, Laboratoire.

Morenon, P., Multon, S., Sellier, A., Grimal, E., Hamon, F. and Bourdarot, E. (2017). "Impact of stresses and restraints on ASR expansion." *Construction and Building Materials*, 140, pp. 58–74.

Multon, S. and Toutlemonde, F. (2006). "Effect of applied stresses on alkali–silica reaction-induced expansions." *Cement and Concrete Research*, 36(5), pp. 912–920.

Pan, J., Feng, Y., Jin, F. and Zhang, C. (2013). "Numerical prediction of swelling in concrete arch dams affected by alkali-aggregate reaction." *European Journal of Environmental and Civil Engineering*, 17(4), pp. 231–247.

Saouma, V. and Perotti, L. (2006). "Constitutive model for alkali-aggregate reactions." *ACI materials journal*, 103(3), p. 194.